doi:10.1093/plphys/kiab366 PLANT PHYSIOLOGY 2021: 187: 1587–1604

Plant Physiology®

Research Article

RBP differentiation contributes to selective transmissibility of *OPT3* mRNAs

Xinmin Lv,[1,†] Yaqiang Sun,[1,†] Pengbo Hao,[1] Cankui Zhang ,[2] Ji Tian ,[3] Mengmeng Fu,[1] Zhen Xu,[1] Yi Wang ,[1] Xinzhong Zhang,[1] Xuefeng Xu,[1] Ting Wu [1,*,‡] and Zhenhai Han [1,‡]

1 State Key Laboratory of Agrobiotechnology, College of Horticulture, China Agricultural University, Beijing, 100193, China
2 Department of Agronomy and Purdue Center for Plant Biology, Purdue University, West Lafayette, Indiana, 47907, USA
3 Plant Science and Technology College, Beijing University of Agriculture, Beijing, 102206, China

*Author for communication: wuting@cau.edu.cn
†These authors contributed equally (X.L., Y.S.).
‡Senior authors.

T.W. and Z.H. conceived and designed the research. Y.S., X.L., P.H., M.F., and Z.X conducted the experiments. J.T., Y.W., X.X., and X.Z. contributed reagents and analytical tools. T.W. and X.L. wrote the manuscript. C.Z gave advice and edited the manuscript. All authors read and approved the manuscript.

The authors responsible for distribution of materials integral to the findings presented in this article in accordance with the policy described in the Instructions for Authors (https://academic.oup.com/plphys/pages/General-Instructions) are: Ting Wu (wuting@cau.edu.cn) and Zhenhai Han (rschan@cau.edu.cn).

Abstract

Long-distance mobile mRNAs play key roles in gene regulatory networks that control plant development and stress tolerance. However, the mechanisms underlying species-specific delivery of mRNA still need to be elucidated. Here, the use of grafts involving highly heterozygous apple (*Malus*) genotypes allowed us to demonstrate that apple (*Malus domestica*) oligopeptide transporter3 (*MdOPT3*) mRNA can be transported over a long distance, from the leaf to the root, to regulate iron uptake; however, the mRNA of Arabidopsis (*Arabidopsis thaliana*) oligopeptide transporter 3 (*AtOPT3*), the *MdOPT3* homolog from *A. thaliana*, does not move from shoot to root. Reciprocal heterologous expression of the two types of mRNAs showed that the immobile *AtOPT3* became mobile and moved from the shoot to the root in two woody species, *Malus and Populus*, while the mobile *MdOPT3* became immobile in two herbaceous species, *A. thaliana* and tomato (*Solanum lycopersicum*). Furthermore, we demonstrated that the different transmissibility of *OPT3* in *A. thaliana* and *Malus* might be caused by divergence in RNA-binding proteins between herbaceous and woody plants. This study provides insights into mechanisms underlying differences in mRNA mobility and validates the important physiological functions associated with this process.

Introduction

Plant grafting is a vegetative propagation technique for horticultural trait improvement, such as stress tolerance, development, and flowering characteristics (Taller et al., 1998; Edelstein et al., 2005; Venema et al., 2008). Experiments with various horticulturally important plant species have shown that abiotic stress can be alleviated by grafting scions to stress-tolerant rootstocks (Rivero et al., 2003; Papadakis et al., 2004a, 2004b; Sanchez-Rodriguez et al., 2012; Wang et al., 2017). Such studies have also revealed that physiological and morphological features can be altered by rootstock–scion interactions (Warschefsky et al., 2015). Grafting-

Received April 29, 2021. Accepted July 11, 2021. Advance access publication August 2, 2021

induced phenotypic changes have been proposed to be associated with the actions of mobile plant hormones, RNAs, and proteins (Haywood et al., 2005; Molnar et al., 2010; Chen et al., 2016), but the underlying mechanisms are not well understood.

Previous studies have shown that grafts involved in two different species or a transgenic plant and its corresponding wild-type (WT) can be used to study long-distance transmission of specific signals (Xia et al., 2018). Grafting experiments have confirmed that endogenous RNA molecules exist in phloem sap (Ham and Lucas 2017) and mRNAs move in both the stock-to-scion and scion-to-stock directions. The long-distance transport of RNAs is facilitated by specific proteins that prevent RNAs from being degraded during transport (Kehr and Kragler 2018). It is known that pumpkin (*Cucurbita maxima*) endogenous proteins PHLOEM PROTEIN 16 (CmPP16) binds to its own RNA to form a ribonucleoprotein (RNP) complex in pumpkin (*C. maxima*). This complex interacts with the plasmodesmata protein, noncell autonomous phloem protein 1, thereby increasing the size exclusion limit of the plasmodesmata that connect companion cells (CCs) and sieve tubes and facilitating entry into the phloem for long-distance transport (Xoconostle-Cazares et al., 1999; Taoka et al., 2007). Proteomic analyses of phloem sap have shown that >10% of total phloem sap proteins are characterized as RNA-binding proteins (RBPs), and it is believed that the binding of phloem-residing RNAs to RBPs may play important roles in loading, unloading, and long-distance transport of RNA in the phloem sieve system (Lin et al., 2009; Rodriguez-Medina et al., 2011; Hu et al., 2016). *Cucurbita maxima* RBP 50 (CmRBP50) from pumpkin has been shown to specifically bind to RNAs harboring the polymer-pyrimidine CUCU domain to form the core of the RNP complex, which then assists long-distance RNA transport in the phloem by binding to additional proteins (Ham et al., 2009). *Solanum tuberosum* polypyrimidine tract-binding protein 1 (StPTB1) and StPTB6, the RBP50 homologs in potato (*S. tuberosum*), have been shown to be able to bind to the 3′-untranslated region (UTR) region of *S. tuberosum* BEL1-like transcription factor (*StBEL5*) mRNA and facilitate long-distance phloem transport of the transcripts to improve tuber yield (Cho et al., 2015).

Enormous amounts of mRNAs have been discovered to be mobile during nutrient stress. For example, a total of 3,546 distinct mRNAs were identified to be transported from a cucumber (*Cucumis sativus*) scion to a watermelon (*Citrullus lanatus*) stock in response to phosphorous deficiency (Zhang et al., 2016b). In another heterografting experiment using two *Arabidopsis thaliana* ecotypes (Columbia-0 [Col-0] and Pedriza-0), although 2,006 different mRNAs were discovered to be mobile in the shoot–root system under normal conditions, only 90 and 91 transcripts were found to be mobile in response to phosphorus (P) and nitrogen (N) deficiency, respectively (Thieme et al., 2015). In addition, Xia and Zhang (2020) established a *Nicotiana benthamiana*/tomato heterograft system to identify shoot-to-root mobile mRNAs that are produced in response to low N, P, or iron (Fe). Although the substantial amounts of mobile mRNAs identified from these studies imply the potential roles of these transcripts in adapting plants to low minerals, a definite biological function of these mRNAs has not been determined.

Fe is an essential micronutrient for plant growth (Brear et al., 2013) and insufficient availability often limits plant development. Previous studies, including physiological (Kobayashi and Nishizawa 2012), transcriptomic (Enomoto et al., 2007), metabolic (Hansch and Mendel 2009), and signal transmission (Mai et al., 2016) analyses, have improved our understanding of mechanisms involved in Fe homeostasis, and substantial evidence exists for shoot-to-root signaling in response to varying Fe conditions (Grusak and Pezeshgi 1996; Enomoto et al., 2007; Wu et al., 2012; Garcia et al., 2013; Grillet et al., 2018). *AtOPT3*, one of the most studied genes related to Fe-deficiency responses, is mainly expressed in vascular tissues and might regulate the long-distance transport and distribution of Fe in *A. thaliana* (Lubkowitz 2011). In the *opt3-2* mutant, the expression of ferric reduction oxidase 2 (*FRO2*) and Fe/Zn/Mn uptake transporter Fe-regulated transporter 1 (*IRT1*) in roots was upregulated and the accumulation of Fe in the roots and leaves increased in comparison with WT, indicating that an *OPT3*-mediated long-distance mobile signal produced in the aboveground parts of the plant negatively regulates the uptake of Fe in roots (Stacey et al., 2008; Zhai et al., 2014). However, the identity of the signal remains elusive and whether the long-distance movement of *AtOPT3* mRNA participates in this regulatory process is unknown.

One of the prerequisites for the identification of mobile mRNAs using the heterografting method is to have a certain degree of genetic difference between the scion and the rootstock (Xia and Zhang 2020). Self-incompatible apple (*Malus*) species have particularly high levels of genetic variation and the use of heterografts of *Malus* species allowed us to investigate the long-distance movement of *Malus domestica* (*Md*) oligopeptide transporter3 (*MdOPT3*) mRNA from the leaf to the root to regulate Fe uptake, and to contrast this with the movement of *AtOPT3* mRNA in *A. thaliana*. These observations were then associated with differences in RBP profiles between *Malus* and Arabidopsis. Our extended studies in tomato and poplar trees suggest that the observed differential in transmissibility of *OPT3* mRNAs may exist between herbaceous and woody plants.

Results

MdOPT3 mRNA moves from shoots to regulate Fe uptake in roots of *Malus* plants

To gain insight into long-distance mRNA signal transduction in apple plants in response to Fe stress, we established a heterologous apple grafting system (Figure 1, A and B). Long-distance movement of RNAs in the shoot–root system was determined using a scion of "Golden Delicious" (*Md*) and two rootstocks: *Malus xiaojinensis* (*Mx*), which is Fe

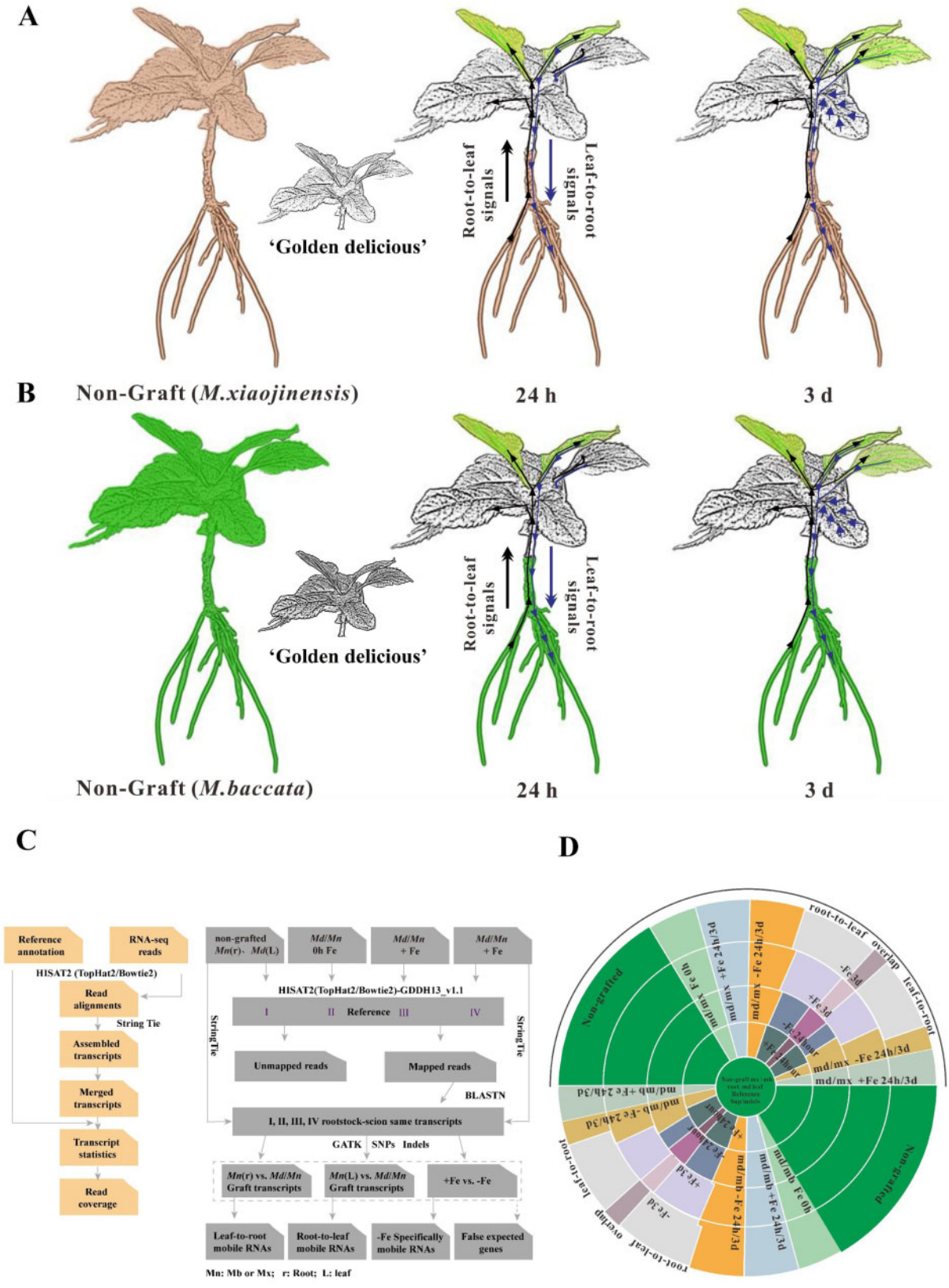

Figure 1 Detection of transmissible mRNAs associated with responses to Fe stress in *Malus*. A, Model of Fe stress signals transported from root to leaf (black arrows) and leaf to root (blue arrows) The brown plant represents the *Mx*. The bright green shading represents the leaves of *Malus* plants. The terms 24 h and 3 d in (A) means the grafted *Md*/*Mx* were treated under +Fe and −Fe nutrient solution for 24 h and 3 d (B) Samples collected from the grafted rootstocks and scions at 0 h, 24 h and 3 d ± Fe treatment (0 h ± Fe treatment means the grafted *Malus* plants were treated under +Fe and −Fe nutrient solution for 0 h. The terms 24 h and 3 d in (B) means the grafted *Md*/*Mx* were treated under +Fe and −Fe

uptake efficient, and *Malus baccata* (*Mb*), which has a much lower Fe uptake efficiency (Zhang et al., 2017). To obtain a profile of the mobile transcripts, we analyzed our previous RNA sequencing (RNA-Seq) data on the hetero-grafted samples (Sun et al., 2020; Figure 1, C and D; Supplemental Table S1). A total of 1,421 distinct mobile mRNAs were identified, of which 14 participated in bi-directional movement. We next searched for transmissible mRNAs that were specifically associated with the Fe-deficiency treatments and identified 193 transcripts, in which 150 moving from leaves to roots and 43 in the opposite direction (Supplemental Table S1). Gene ontology (GO) enrichment analysis showed that the mRNAs moving from leaves to roots were enriched in the "transport" (GO: 0006810), "response to stress" (GO: 0006810), and "biosynthetic process" (GO: 0009058) pathways (Supplemental Figure S1).

Using the population of the specifically transmissible mRNAs, we performed a weighted gene co-expression network analysis and identified 14 distinct modules (Supplemental Figure S2). One of the 14 modules is closely related to the Fe-deficiency response and was of particular interest for this study (purple module). Further exploration of the Fe-associated module showed that *OPT3* has high connectivity to other members in the network, indicating the possibility of this transcript in a wide range of Fe regulatory pathways (Figure 2A; Supplemental Table S2). The abundances of *MdOPT3* transcripts were found to be more significantly accumulated in roots of *Md/Mx and Md/Mb* grafts subjected to Fe-deficiency treatment than those in control condition. Interestingly, this overaccumulation of *MdOPT3* transcripts in roots coincided with the reduced accumulation of the same transcripts in leaves (Figure 2B). We next performed RNA fluorescence in situ hybridization (FISH) and localized the *MdOPT3* mRNA to be in the phloem in stem cross-sections, whereas in root, *MdOPT3* mRNA signal appeared to be unloaded and diffused to all vascular bundle cells (Figure 2C). Since *OPT3* has been linked to phloem-specific Fe transport in *A. thaliana* (Stacey et al., 2002, 2008; Zhai et al., 2014), we then tested whether it is involved in Fe accumulation in *Malus*. We found that *MdOPT3* transient suppressed *Malus* plant grown under normal Fe or Fe-deficient conditions showed weaker Fe^{3+} staining and a significant decrease of Fe contents compared with the control plants (Figure 2, D and E). This suggested that the *MdOPT3* contributes to the coordination of Fe accumulation in *Malus* plant.

To further validate *MdOPT3* mRNA mobility in *Malus* grafts, we analyzed the *OPT3* gene sequences from cv "Golden Delicious," *M. xiaojinensis*, and *Mb*. A single-nucleotide polymorphism (SNP) (T/C) was identified at +995-bp downstream from the ATG start site, comprising a $MdOPT3^{T}$ allele present in "Golden Delicious," a $MbOPT3^{C}$ allele in *Mb*, and an *Mx* oligopeptide transporter 3 ($MxOPT3^{T/C}$) allele in *M. xiaojinensis* (Figure 3A; Supplemental Figure 3A). A combination of *OPT3* homozygous genotypes of "Golden delicious" ($MdOPT3^{T}$) and *Mx* ($MbOPT3^{C}$) allowed us to distinguish the origin of *OPT3* in *Md/Mb* grafts accurately. In this heterograft, the $MdOPT3^{T/C}$ was identified in roots under normal growth conditions (Figure 3B). However, after Fe-deficiency treatment of grafted seedlings, $MdOPT3^{T}$ was the only form of transcript detected in the roots of *Md/Mb* grafts (Figure 3B). This showed that, under Fe-deficient growth condition, the expression of the root-derived *OPT3* was prohibited and the detected *OPT3* in the root originated from the scion via the leaf-to-root long-distance movement.

The movement of nutrients and signaling molecules from the leaf-to-root normally take place in phloem (Aloni et al., 2010; Aoki et al., 2005; Kehr and Buhtz 2008). To further verify whether $MdOPT3^{T}$ is mobile from the leaf-to-root in the *Malus* grafts, phloem girdling, a technique that disrupts the phloem transport, was employed. The expression of *MdOPT3* in the girdled plant was barely detected. In addition to *MdOPT3*, we also analyzed the abundance of *MdWOX13* (homologous gene of *PbWOX1*) in the girdled plant. *PbWOX1* was previously reported to be mobile in pear (Duan et al., 2015). Its homologous gene *MdWOX13* has also been detected to be mobile in our study. The significantly reduced abundance of WUSCHEL-related homeobox 13 (*WOX13*) mRNA in the roots of the girdled *Md/Mb* heterografts indicated that our observation on *MdOPT3* was not a coincidence (Figure 3C). This result indicated that the $MdOPT3^{T}$ mRNAs were indeed originated from the leaf and transported from the *Md* scion to the *Mb* rootstocks via the phloem.

AtOPT3 mRNA does not move from shoots to roots in *A. thaliana*

AtOPT3 was shown to promote the movement of Fe from xylem to phloem in *A. thaliana* and regulate the redistribution of Fe signal and associated signaling in developing and mature tissues (Mendoza-Cozatl et al., 2014). The discovery

Figure 1 (Continued)

nutrient solution for 24 h and 3 d. The nongrafted control samples were collected from *Mx*/*Mb* roots and *Md* leaves. The green plant represents the *Mx*. C, Design of the micro-graft experiments and experimental strategy. Modular bioinformatics schematic using RNA-seq data in *Malus*. The yellow module represents the alignment flow between reads and the reference genome in the root and leaf of the grafted sample, and the grey module represents the transfer mRNA identification flow. First, the clean data from stock or scion of the four samples were compared with the reference genomic GDDH13V1.1 to obtain the modified genome sequence (I\II\III\IV) of each sample. Second, mapped reads were turned into Merged seq transcripts by using the method of BLASTN. The GATK was used to annotate the SNP changed reads of each sample. When determining leaf-to-root mobile genes, the genes that retain the SNP (heterozygosity of rootstock loci) consistent with scions were screened. The accuracy of a SNP is judged according to the sequencing depth and the number of sample repeats. *Mn* stands for *Mb* or *Mx*, r: root, L: Leaf. HISAT2: graph-based alignment of next generation sequencing reads to a population of genomes (D) Specific screening methodology. SNPs between different samples were used to identify transmissible mRNAs. The different colors indicate total SNPs after comparison with reference genome.

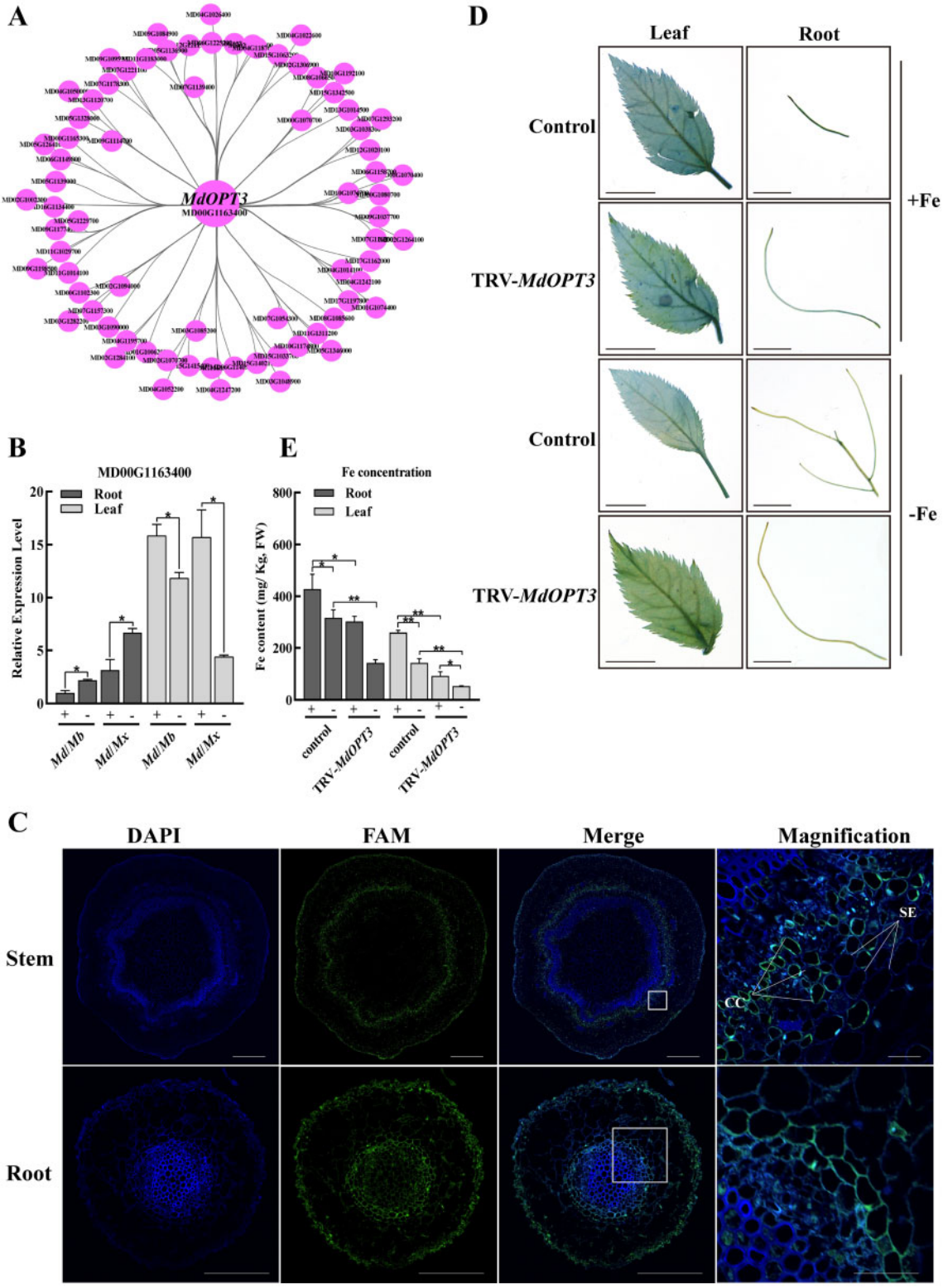

Figure 2 The potentially mobile RNA *OPT3* response to Fe deficiency in *Malus* plants. A, Weighted correlation network analysis (WGCNA) the mobile RNA response to Fe deficiency. B, Relative expression level of *MdOPT3* (MD00G1163400) in *Md*/(*Mx and Md*/*Mb* grafted seedlings under +Fe and −Fe treatments. C, RNA FISH of *MdOPT3* in *Mb* stem and root. The sections of stems and leaves stained with nuclear dye DAPI appear blue. The green fluorescence indicates the expression site of the target gene *MdOPT3*. The length of the ruler in the field of view of DAPI, FAM, and Merge is 200 μm. The length of the ruler in the field of view of Magnification is 20 μm. SE, sieve elements. The white box indicates the enlarged part (D) Perls' staining of leaves and roots from transient transgenic *Md* seedlings. Analysis of Fe distribution was performed using Perls' staining. Scale bars: 1 cm. E, Fe concentration in roots and leaves of *MdOPT3*-suppressed *Malus* plants. B and E, Values are means ± SD ($n = 3$), *Statistically significant difference ($P < 0.05$), **extremely statistically significant significant difference ($P < 0.01$), as determined by a Student's *t* test.

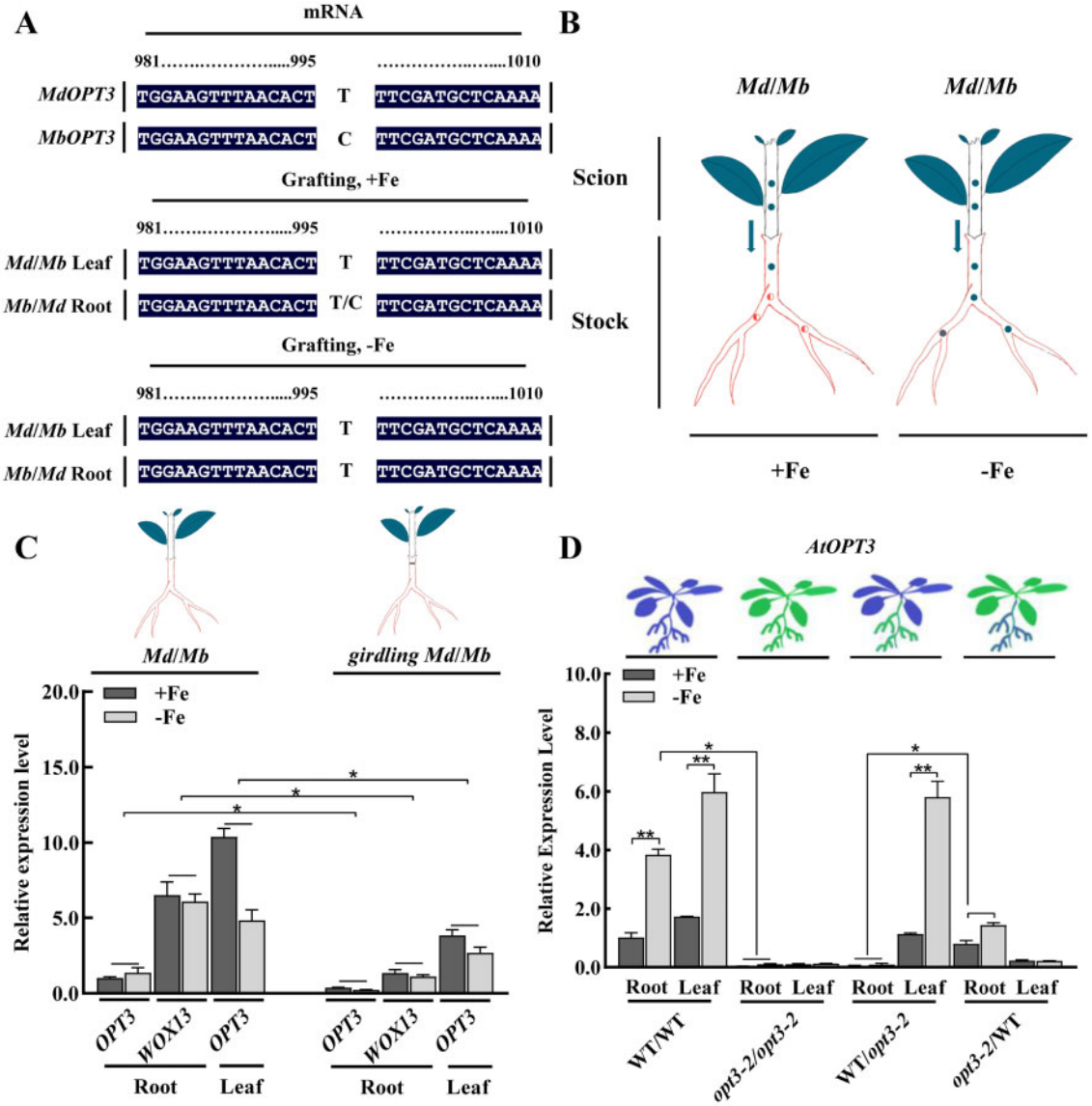

Figure 3 *OPT3* is a mobile mRNA in *Malus* Plants, but not in Arabidopsis. A, A stable SNP (+995 bp) site was found through the *OPT3* sequence alignment between *Md and Mb*. The SNP site in the root and leaf of *Md*/*Mb* grafted seedlings changed after grafting under +Fe and −Fe treatments. B, The stable SNP site was used to identify the mobility of *OPT3* from shoot to root in the *Md*/*Mb* graft complexes under +Fe and −Fe treatments. Circles of different shapes and colors represent different SNP sites in different *OPT3* ($MdOPT3^{T}$,$MbOPT3^{C}$). The arrow indicates that the *MdOPT3* in the leaf can move to the root. C, Effect of girdling on the expression of *OPT3* in roots of *Md*/*Mb* grafted seedlings under +Fe and −Fe treatments. *WOX13* was used as the positive control for this experiment. Two schematic diagrams, respectively, show un-girdled and girdled apple grafted seedlings. (D) The relative expression of *AtOPT3* in Arabidopsis graft complex (WT/WT, *opt3-2*/*opt3-2*, WT/*opt3-2*, and *opt3-2*/WT) shoots and roots under +Fe and −Fe treatments. In the diagram, the blue plants represent WT *A. thaliana*, and the green plants represent the *opt3-2* mutant. Different colors of Arabidopsis leaves and roots represent different grafting combinations. C and D, Values are means ± SD ($n = 3$), *Statistically significant difference ($P < 0.05$), **extremely statistically significant difference ($P < 0.01$) as determined by a Student's *t* test.

of the movement of the *Malus OPT3* inspired us to investigate whether the long-distance movement of the *OPT3* mRNA is a common phenomenon in plants. We reciprocally grafted shoots of the *AtOPT3* knockdown mutant (*opt3-2*) onto WT rootstocks (*opt3-2*/WT) and WT shoot scions onto *opt3-2* rootstocks (WT/*opt3-2*), and determined *AtOPT3* expression in the two graft combinations. Compared to the WT/WT control, the expression of *AtOPT3* was hardly detected in the roots of WT/*opt3-2* (Figure 3D), indicating that the *AtOPT3* mRNAs in WT leaves were not transported to the *opt3-2* roots in Arabidopsis.

The mechanistic basis of the differences in *OPT3* mRNA mobility between herbaceous and woody plant species

The above results showed that *OPT3* mRNAs from *A. thaliana and Malus* plants differ in their mobility. The alignment

analysis between *MdOPT3* and *AtOPT3* showed that the two sequences share 73% identity at the cDNA level. To determine whether the mRNA sequence differences affect their mobility, transient expressions of *MdOPT3* in *A. thaliana* rosette leaves or *AtOPT3* in apple leaves were conducted (Figure 4). PCR primers that can distinguish the two transcripts were used to measure the expression levels of *OPT3* in the roots of control and transient transgenic plants (Supplemental Table S3). We found that *AtOPT3* mRNAs could be detected in the roots of the transient transgenic apple seedlings but not in the control, although *AtOPT3* mRNA levels in apple roots were lower than those in the shoot (Figure 4). In contrast to the results from the transient transgenic apples, the *MdOPT3* transcripts could not be detected in the Arabidopsis roots although the transcripts could be detected in high abundance in leaves with a previously described mobile mRNA *A. thaliana* translationally controlled tumor protein 1 (*AtTCTP1*; Yang et al., 2019) as a positive reporter (Figure 4). To confirm the efficiency of the mobile mRNA detection in Arabidopsis using transient expression, we also conducted the transient expression of the known mobile mRNA *AtTCTP1* fused to *eGFP* in Arabidopsis rosette leaves. We found that e*GFP-AtTCTP1* mRNAs could be detected in the roots of the transient transgenic Arabidopsis seedlings but not in the control (Supplemental Figure S4). Taken together, these results indicated that factors other than the sequence specialty of *OPT3* conferred the differential shoot-to-root mobility in the two species.

In plants, RBPs play a key role in mRNA transport (Singh et al., 2015), and the 3′-UTR of mobile mRNAs was demonstrated to be sufficient for the long-distance movement of various mRNAs. To identify putative *MdOPT3* RPBs, we used a 3′-UTR *MdOPT3* sequence as a probe (Figure 5A), and performed RNA-pull down coupled with mass spectrometry. A total of 911 proteins from *Md* were identified to be able to interact with *MdOPT3* mRNA (Supplemental Table S4). The candidate proteins were functionally annotated and a GO enrichment analysis revealed that the most enriched category belongs to "response to stimulus" (Figure 5B). These 911 proteins included five RBPs: MD04G1208800, MD12G1223200, MD05G1230700, MD07G1160000, and MD14G1031800 (Figure 5, C and D), of which MD04G1208800 and MD12G1223200 expression were upregulated in roots of both *Md/Mx and Md/Mb* grafted seedlings subjected to Fe-deficiency treatment (Figure 5C).

To quantify the binding affinities of *Malus and A. thaliana* RBPs with their associated mRNAs, we used surface plasmon resonance (SPR) assays with immobilized oligonucleotides. We expressed five *Malus* RBPs and the corresponding *A. thaliana* proteins in *Escherichia coli*, each as a fusion with glutathione S-transferase (GST), and purified the recombinant fusion proteins (Figure 6A). The two *Malus* RBPs (MD04G1208800 and MD12G1223200) were found to be bound to the 3′-UTR of the *MdOPT3* and *AtOPT3* probes with high affinity, whereas the corresponding *A. thaliana* RBP (AT3G26420.1) had a much lower binding value than the *Malus* RBPs, suggesting the low affinity of the *A. thaliana* RBP with the 3′-UTR of the *MdOPT3 and AtOPT3* probes (Figure 6, B–D). To investigate whether RBPs contribute to *MdOPT3* mRNA mobility, we studied the role of RBPs with a transient expression system in which tobacco rattle virus (TRV) was employed to silence *RBP* expression in the apple seedlings. We then grafted shoots of the *MdRBP* transiently suppressed *Malus* onto WT rootstocks, and determined *MdOPT3* expression in the roots. Our analysis showed that *MdOPT3* transcripts were barely detected in the apple roots (Supplemental Figure S5). This result showed that the mobility of *MdOPT3* may be associated with the characteristics of the MdRBP in apple. To verify whether the mobility of the *AtOPT3* can be increased if the MdRBPs are present in Arabidopsis, we overexpressed *MdRBP* in the Arabidopsis CCs and grafted this transient transgenic plant on the *opt3-2* mutant rootstock (*AtSUC2::MdRBP/opt3-2*). Compared to the WT/*opt3-2* control, the expression of *AtOPT3* was detected at much higher abundance in the roots of *AtSUC2::MdRBP/opt3-2* (Supplemental Figure S6). This result not only validated the relationship between the mobility of *MdOPT3* and the presence of MdRBPs in apple, it also indicated that the lack of mobility of *AtOPT3* in Arabidopsis may be due to the absence of a compatible AtRBP.

In order to find out whether the above findings also apply to other plant species, we conducted transient expressions of *MdOPT3* in *Solanum lycopersicum* leaves and *AtOPT3* in *Populus tremula* leaves (Supplemental Figure S3B). Similar to our discovery in the *Malus* transient expression study, we found that *AtOPT3* mRNAs could be detected in the roots of the transient transgenic *P. tremula* (Supplemental Figure S3C). On the contrary, the *MdOPT3* transcripts could not be detected in roots of transient transgenic *S. lycopersicum* although the transcripts were in high abundance in leaves (Supplemental Figure S3C). These results led us to speculate that the differences between *A. thaliana* and apple in the transmissibility of *OPT3* mRNAs may also be associated with the different functions of the RBP proteins present in other herbaceous plants and woody plants.

To validate whether special sequence motifs associated with their RBPs exist in herbaceous and woody plants, we performed a multiple sequence alignment of RNA binding domain (RRM) of RBPs (MD12G1223200 and MD04G1208800) from multiple herbaceous and woody plant species. Our analysis discovered that the RRM of the RBPs formed separate clusters between herbaceous and woody plants and showed the presence of the conserved "AA" at the 76–77th amino acid site in most herbaceous species, whereas these two amino acids were replaced by "EE" or "EA" in most woody plants (Figure 5E; Supplemental Figure S7). Whether the difference of the two amino acids in the RBPs is associated with *OPT3* mobility is worth of future exploration.

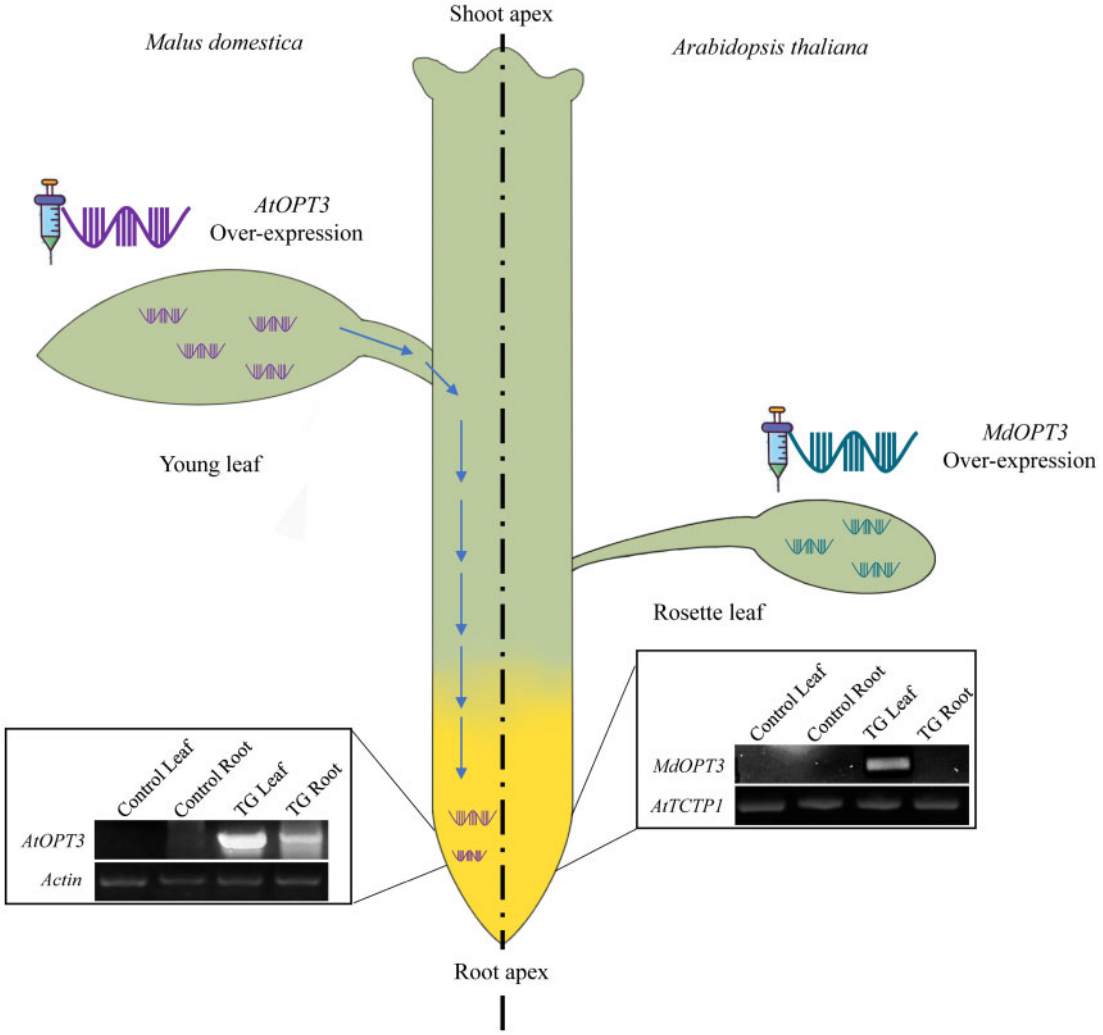

Figure 4 Using transient transformation of heterologous *OPT3* expression in *Malus* plant and Arabidopsis to identify the mobility difference of *OPT3* between *Malus* plant and Arabidopsis. The expression of heterologous *OPT3* was detected by RT-qPCR in the roots of transient transgenic plants, and the untransformed plants were used as controls. *AtTCTP1* specifically expressed in the phloem of *A. thaliana* was used as the positive control of this experiment. TG, transgenic plant. The dashed-dotted line divides the schematic plant into left and right parts. The left side represents the *Md*, and the right side represents the *A. thaliana*. The green portion of the plant represents the shoot, and the yellow portion of the plant represents the root. The blue arrows mean that *AtOPT3* can move from the transiently transgenic apple leaf to the root. Large RNA indicates mobile mRNA which transport from leaves, while small RNA indicates the local mRNA which express in roots.

Mobile *MdOPT3* mRNAs are required for the Fe-deficiency response in *Malus* plants

It was previously reported that Arabidopsis mutant *opt3-2* exhibited a constitutive Fe-deficiency response in the root (Zhai et al., 2014). Consistent with this early finding, our results showed that the expressions of the *IRT1 and FIT* in roots of the *opt3-2* mutant were constitutively upregulated, indicative of an Fe-deficiency response (Supplemental Figure S8, B and D). To confirm *MdOPT3* is the functional homolog of the Arabidopsis *AtOPT3*. We evaluated the phenotypes of the transient Pro*AtOPT3*::*MdOPT3*-expressing lines. Since the Arabidopsis mutant *opt3-2* shows a constitutive Fe-deficiency response in roots including the upregulation of FCR, *A. thaliana* Fe-regulated transporter 1 (*AtIRT1*) and *A. thaliana FRO2* (*AtFRO2*) *AtFRO2*, we tested whether expression of *MdOPT3* was able to complement both phenotypes. We found that in FCR activity, *AtIRT1 and AtFRO2* expressions were greatly reduced in the roots of Pro*AtOPT3*::*MdOPT3* expressing plants compared to the *opt3-2* mutant (Supplemental Figure S9). These results show that *MdOPT3* is sufficient for proper regulation of Fe homeostasis and apple *MdOPT3* is indeed the homolog of the Arabidopsis *AtOPT3*. To explore whether *MdOPT3* is involved in Fe-deficiency responses in apple plants, we measured the expression levels of the two Fe-deficiency marker genes, *MdIRT1 and MdFIT*, in transient *MdOPT3* suppressed apple plants. To our surprise, both *IRT1* and *FIT* were downregulated in the suppressed plants when compared with the control plants (Supplemental Figure S8, F and G). The contrast response to the suppressed expression of *OPT3* in leaf between *Malus* and Arabidopsis inspired us to hypothesize that *OPT3* mobility could play a role in this physiological process.

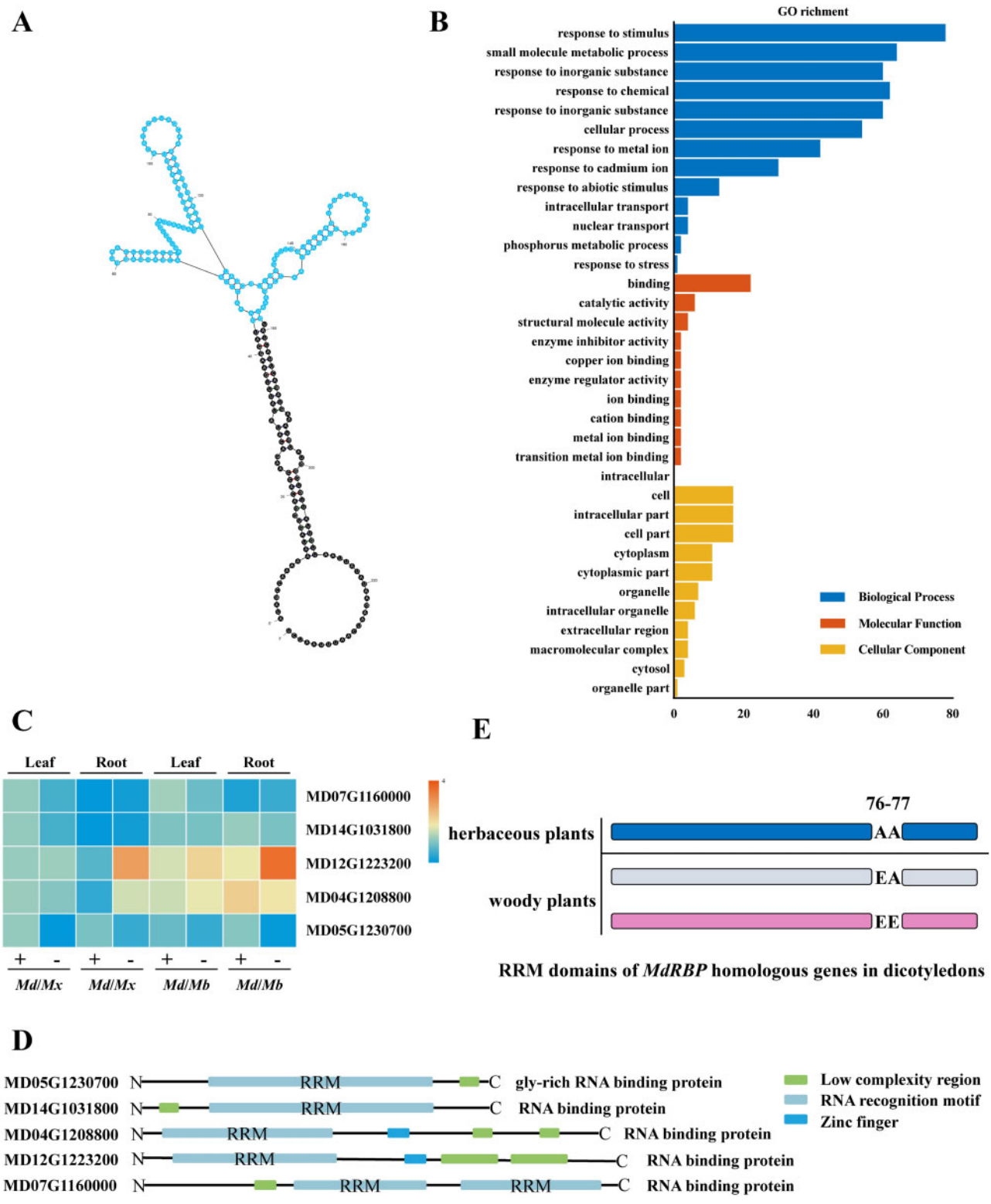

Figure 5 Analysis of proteins that interact with *MdOPT3* 3′-UTR. A, Analysis of the secondary structure of *MdOPT3* 3′-UTR sequence. Different numbers indicate different base sequences of *MdOPT3* 3′-UTR. The blue circle represents the sequence that can form a tRNA-like structure, and the black circle represents the rest of sequence. B, GO enrichment analysis of proteins interacting with *MdOPT3* 3′-UTR sequence. The *X*-axis represents the number of genes enriched in GO. C, Candidate RBPs relative expression levels in roots and leaves of *Md*/*Mx and Md*/*Mb* graft complexes under +Fe and −Fe treatments. Color bar in the heat map indicate the level of gene expression (D) Candidate RBP domain analysis. RRM: RNA recognize motif. The thick black line in the figure indicates the amino acid sequence that cannot form a specific domain. E, RRM domain analysis of two RBPs in herbaceous and woody plants. Gray and pink strips indicate two RBP proteins with different amino acid sequence in woody plants. The numbers 76–77 in the figure represent the 76–77th amino acids of the RBP protein. AA, AE, and EE, respectively, indicate that the amino acids at positions 76–77 are alanine–alanine, alanine–glutamate, and glutamate–glutamate.

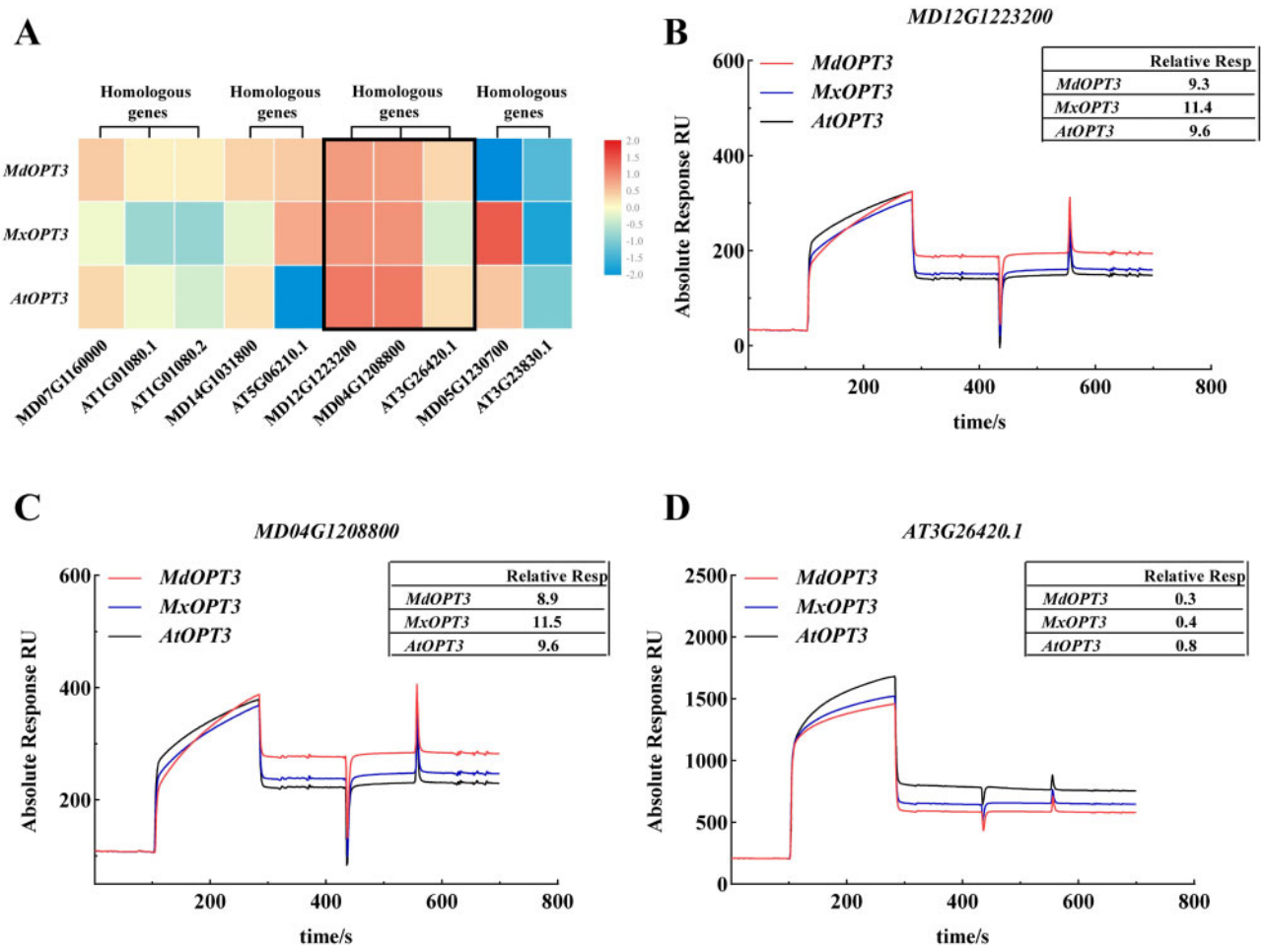

Figure 6 SPR analysis of the binding of candidate RBPs to *MdOPT3*, *MxOPT3*, and *AtOPT3* 3′-UTR. A, The binding of candidate RBPs with the *MdOPT3*, *MxOPT3*, and *AtOPT3* 3′-UTR sequences was tested and the response curves of three RBPs, (B) MD12G1223200, (C) MD04G1208800, and (D) AT3G26420.1 to the *MdOPT3*, *MxOPT3*, and *AtOPT3* 3′-UTR sequences are shown. The different colored squares in the heat map and the black table in the figure parts (B–D) indicate the level of binding ability of the RNA probe to the RBP protein, expressed in terms of Absolute Response RU. The black box in the figure indicates the proteins that can obviously interact with the RNA probe.

It is known that *OPT3* is located on the vascular tissues of both roots and shoots (Zhai et al., 2014). To distinguish the importance of leaf and root *AtOPT3* in response to Fe deficiency, a few graft combinations, that is, *opt3-2*/WT, *opt3-2*/*opt3-2*, and WT/*opt3-2*, were created and the expressions of *IRT1*, *FIT*, and *FRO2* in roots were measured. Higher expression levels of the marker genes were found in both *opt3-2*/WT and *opt3-2*/*opt3-2*, whereas WT/*opt3-2* grafts had lower expressions of these genes (Figure 7, A–C). These results indicated that the Fe-deficiency responses in Arabidopsis roots were stimulated by a signal from the shoot mediated by OPT3 but *OPT3* transcript is not the mobile signal. To investigate whether the *MdOPT3* mRNA could be the mobile signal in apple plants under Fe-deficiency, it is important to create some *Malus* plants without the mobile *OPT3*. We analyzed the 3′-UTR of *OPT3* from *Mx*, *Mb*, and *Md*, and identified a deletion of 15 bp specific to *MxOPT3* in *Mx* (Supplemental Figure S3A). We observed that *OPT3* mRNAs in *Mx* leaves were immobile, whereas *OPT3* mRNAs in *Mb* leaves were mobile (Supplemental Figure S10). The variation in transmissibility of *OPT3* mRNAs between *Mx and Mb* was used to investigate whether *OPT3* mRNAs mobility contribute to Fe-deficiency response. We created two graft systems, taking *Md* as the rootstock, and *Mx* or *Mb* as the scion (Figure 7, D–G). The lack of the *Mx* derived $OPT3^{C}$ mRNA in the rootstock *Md* indicated the mRNA in the *Mx* leaves could not be transferred to the roots, whereas the detection of the *Mb* derived $OPT3^{C}$ mRNA in the rootstock *Md* indicated that the mRNA in the *Mb* leaves could be transferred. We found the expressions of Fe uptake-related gene (*IRT1*, *FRO2*) were much higher in the *Mb*/*Md* grafts in which *OPT3* was mobile in comparison with the expression in the *Mx*/*Md*, in which the *OPT3* transcript was not mobile. Interestingly, we did not observe significant differences in the expression of *FIT* in both *Mb*/*Md and Mx*/*Md*, indicating that the *MdOPT3* mobility is not involved in the transcriptional regulation of Fe uptake. Taken together, our results showed that the long-distance movement of *OPT3* mRNA from shoots-to-roots involves in Fe uptake in roots of *Malus* plants.

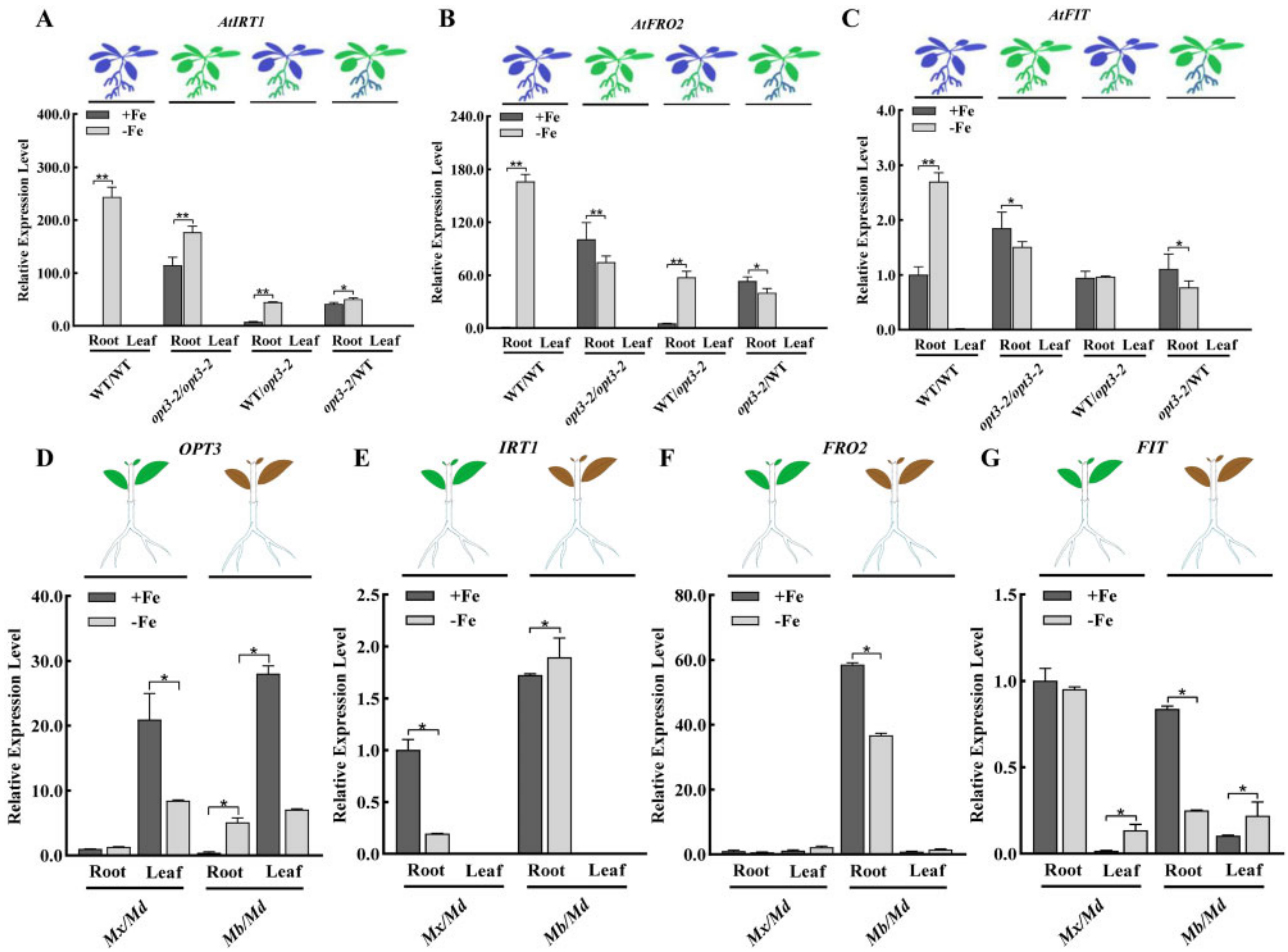

Figure 7 *OPT3* moves from shoots to regulate Fe-deficiency response in roots of *Malus* plants. The relative expression of (A) *AtIRT1*, (B) *AtFRO2*, and (C) *AtFIT1* in Arabidopsis graft complex (blue color plant: WT/WT, green color plant: *opt3-2*/*opt3-2*, blue/green plant: WT/*opt3-2*, green/blue plant: *opt3-2*/WT) shoot and root under +Fe and −Fe treatments. The relative expression of (D) *OPT3*, (E) *IRT1*, (F) *FRO2* and (G) *FIT* in reverse graft complex (green color plant: *Mx*/*Md*, brown color plant: *Mb*/*Md*) leaf and root under +Fe and −Fe treatments. A–G, Values are means ± SD ($n = 3$). *Statistically significant difference ($P < 0.05$), **extremely statistically significant difference ($P < 0.01$), as determined by a Student's *t* test.

Discussion

Based on the data presented in this study, we propose a model regarding the mobility of *OPT3* mRNA in *Malus* and Arabidopsis plants (Figure 8). *MdOPT3* moves long distance from shoots to regulate Fe uptake in roots of *Malus* plants while this is not the case in Arabidopsis. We further provided evidence to demonstrate that the differential transmissibility of *OPT3* in Arabidopsis and *Malus* might represent a generic phenomenon in herbaceous and woody plants although further experiments are needed before these conclusions can be generalized.

At the genome level, various graft-transmissible mRNA putative orthologs were found to be shared among different plant species; however, each plant has a unique phloem mRNA population. For example, 2,006, 3,333, and 3,546 graft-transmissible mRNAs were identified in *A. thaliana*, grape (*Vitis vinefera*), and cucumber phloem, respectively (Thieme et al., 2015; Yang et al., 2015; Zhang et al., 2016b), but only 38% and 33% of the mobile mRNA putative orthologs from *A. thaliana* and grape, respectively, were also detected in cucumber (Zhang et al., 2016b). The core sieve tube system (STS) mRNAs may play roles that are essential for phloem function and therefore are conserved during plant vascular tissue evolution. Conversely, the species-specific STS-mRNAs may reflect differences in growing conditions, or evolutionary adaptations, such as those exhibited by rosette plants (*A. thaliana*), annual plants and perennial vines (grape; Ham and Lucas 2017). The difference in the transmissibility of *OPT3* between apples and *A. thaliana* may be related to differences in the development of vascular bundles, and specifically phloem, between herbaceous and woody plants. In addition to *Malus* and Arabidopsis, we further selected two other herbaceous and woody plants which demonstrated that the originally immobile *AtOPT3* can be transported from the shoot to the root in *P. tremula*, while the originally mobile *MdOPT3* does not show such movement in *S. lycopersicum*. Multiple factors, for example, expression site, association with RBPs, and so on have been suggested to be associated with the mobility of mRNAs (LeBlanc et al., 2013; Kim et al., 2014; Morris 2018). The

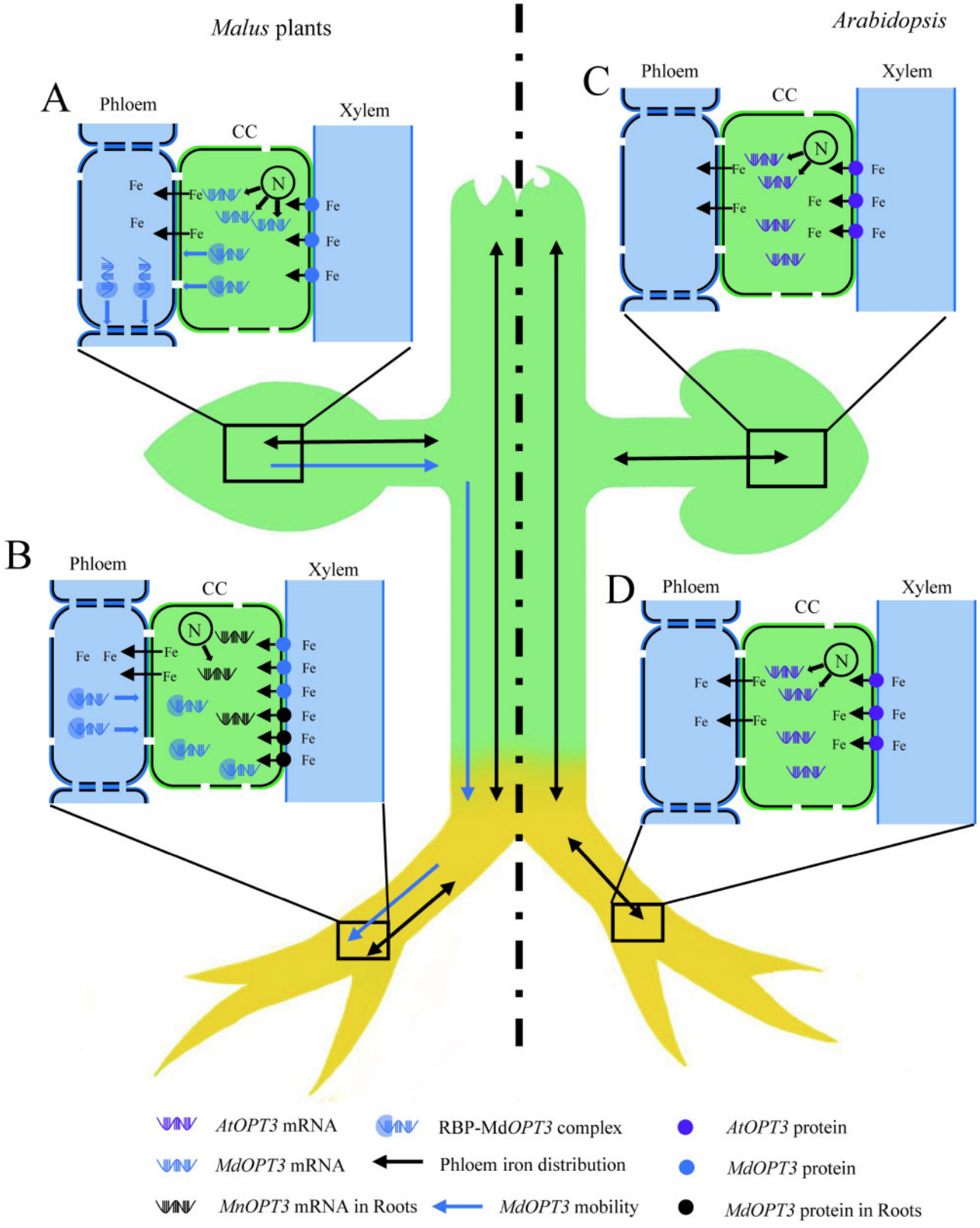

Figure 8 Schematic overview of *OPT3* mobility from shoot to root in *Malus* plants (left) and *A. thaliana* (right). *OPT3* mRNA mobility leads to differences in Fe redistribution between *Malus* plants and *A. thaliana* roots. A, *OPT3* mRNAs in *Malus* shoots are transported to roots by binding to RBPs. B, *OPT3* mRNAs detected in *Malus* roots include sequences endogenous to the root, as well as *OPT3* mRNAs transferred from the shoot. The *OPT3* from shoot and *OPT3* in root jointly participate in the Fe redistribution within the root (from xylem to phloem). C and D, *A. thaliana* *OPT3* mRNAs are not transported from the shoot to the root. Blue cells indicate phloem and xylem, green cells indicate CC. N means nucleus. The green part represents the shoot, and the yellow represents the root.

noncell-autonomous phloem RBP CmPP16 has been shown to bind to mRNAs in a nonspecific manner, increase the plasmodesmata size exclusion limit, and transmit as an RNP complex between cells (Xoconostle-Cazares et al., 1999). Phloem sap proteomic analysis showed that >10% of phloem sap consists of RBP proteins, which may play an important role in the long-distance transport of RNA in the phloem (Lin et al., 2009; Rodriguez-Medina et al., 2011; Hu et al., 2016). Thus, it is legitimate to assume that the variation in RBP orthologs between apple and *A. thaliana* may contribute to differences in phloem transcript profiles between the two species.

Potato *StBEL5* mRNA was shown to move via the phloem in the veins to the tip of the subsurface stolon (Banerjee et al., 2006; Hannapel 2010), and increasing the long-distance transmission was able to improve tuber yield (Banerjee et al., 2006). The UTR of *StBEL5* was found to be related to its long-distance transmission and other studies also have shown the importance of the 3′-UTR in binding to RBPs for long distance RNA movement (Ferrandon et al., 1994). We analyzed the 3′-UTR of *OPT3* from *Mx*, *Mb*, and *Md*, and identified a deletion of 15-bp specific to *MxOPT3* (Supplemental Figure S3A). We observed that *OPT3* mRNAs in *Mx* leaves were mobile whereas *OPT3* mRNAs in *Mb* leaves were immobile. The variation in transmissibility of *OPT3* mRNAs between *Md*, *Mx*, and *Mb* may reflect variation in the 3′-UTR sequences. It was demonstrated that a potential secondary structure motif resembling tRNA in the 3′-UTR is sufficient for long-distance mRNA movement (Zhang et al., 2016a). The deletion of 15 bp in the 3′-UTR in *Mx* may affect the tRNA structure of *MxOPT3*. Moreover, our results show that variation in the 3′-UTR sequences may affect the mobility of the *mRNA*, which might represent a general tool for precisely regulating communication between scion and rootstock.

The plant *OPT3* gene was first described in *A. thaliana* (Stacey et al., 2002), and in subsequent studies of its function the focus was mainly on the tissue localization of expression changes as a consequence of Fe deficiency, as well as the identification of *opt3-2* mutants (Stacey et al., 2006). It was also found that *AtOPT3* is a key component of the Fe-signaling network connecting shoots to roots (Zhai et al., 2014). Through phloem localization and radioactive Fe tracer tests, *OPT3* were shown to mediate the transport of Fe or Fe ligand complexes from the xylem to the CCs and then to the phloem for long-distance transport (Zhai et al., 2014). Even though phloem RNAs are known to play important developmental roles (Haywood et al., 2005; Rodriguez-Medina et al., 2011; Zhang et al., 2016b), and *AtOPT3* is mainly transcribed and expressed in the phloem (Stacey et al., 2006; Mendoza-Cozatl et al., 2014; Zhai et al., 2014), through an interactive grafting test involving *opt3-2* and WT, we found no evidence that the *OPT3* mRNA can move from the shoot to the root in *A. thaliana* and conclude that the factor mediating the Fe signal transduction from shoot to root in Arabidopsis is less likely the mRNA form of *OPT3*.

To show the overlap of differential regulation in both *opt3-2* and TRV-*MdOPT3 lines*, we compared RNA-seq profiling between *opt3-2* and TRV-*MdOPT3* (Supplemental Table S5). About 43 (root) and 47 (leaf) of the GO pathways were shared in both *opt3-2* and TRV-*MdOPT3* lines. A large proportion of the common enriched terms are related to "response to iron," "iron chelate transport," "response to hormone" category, and so on (Supplemental Figure S11). Different from Arabidopsis, mobile *MdOPT3* mRNA is required for the Fe-deficiency response in *Malus* plants. Our results showed *MdOPT3* mRNA acts as a Fe signal transduced from shoot to root. It is unknown why the shoot-to-root movement of *OPT* mRNAs is needed and how the root-arriving *OPT3* participates in the Fe-deficiency responses. Small peptides have diverse functions in cellular signaling in many organisms (Murphy et al., 2012; Endo et al., 2014; Luo et al., 2019). In addition to Fe, OPT proteins can transport diverse substrates which are peptide-containing compounds or peptide derivatives. Also, we speculated that scion-originated *OPT3* may deliver into the specific terminal regions of the root which is different from the localization of the root-originated *OPT3*. Future experiments are needed to verify whether the oligopeptide transport function plays a role in regulating Fe-deficiency response in *Malus* plants.

Materials and methods

Plant materials

Malus xiaojinensis and *Mx* as rootstocks, and *Md* cv "Golden Delicious" as scion were propagated on Murashige and Skoog (MS) medium (Gao et al., 2011) containing 0.5 mg L^{-1} 6-benzylaminopurine and 0.5 mg L^{-1} indole-3-butytric acid for 1 month (growth temperature 25 ± 2°C day/21 ± 2°C night, 250 μmol m^{-2} s^{-1} light intensity, 16-/8-h light/dark photoperiod). The seedlings were transferred to MS medium with 1.0 mg L^{-1} indole-3-butytricacid for rooting (Han et al., 1994). Seedlings were grown for 3 weeks prior to experimental treatments. Fe sufficient (+Fe) or Fe-deficient (−Fe, 0 μM FeNaEDTA) treatments were carried out for 3 d.

Arabidopsis thaliana lines included WT (Col-0) and *OPT3* knockdown mutants (*opt3-2*) (Stacey et al., 2008). The seeds were surface-sterilized, stratified at 4°C for 48 h in the dark, and seeded on solid half MS medium (pH 5.8) with an aseptic pipette suction head under sterile conditions. The plates were then placed at room temperature (16-/8-h light/dark cycle, temperature 22°C) and cultured vertically for 6 d. +Fe and −Fe media were prepared as previously described (Khan et al., 2018).

Plant grafting

Before grafting, *Malus* plants were grown in MS medium for 1 month in a controlled environment as described above. Rootstocks and scions with similar stem diameters were selected for cleft grafting (Melnyk 2017), and the grafted materials were transferred to rooting medium (0.5 mg L^{-1}

indole butyric acid). After one and a half months, the grafted plants were used for Fe-deficiency treatment in hydroponic culture as described above. *Arabidopsis thaliana* grafting was performed using a flat surface collar-free method as previously described (Marsch et al., 2013). Grafting combinations were as follows: WT Col-0/WT Col-0, *opt3-2*/*opt3-2*, WT Col-0/*opt3-2*, and *opt3-2*/WT Col-0.

Phloem girdling

The stems of hydroponically rooted *Md*/*Mb* grafted seedlings were used for the girdling experiments. The bark 2 mm above the graft joint was removed. The girdling part was wrapped with plastic wrap to prohibit water loss. To prevent the healing of the girdling incision, the seedlings after girdling were immediately treated with +Fe and −Fe.

Mobile mRNA bioinformatic analysis

Total RNA was extracted from grafted tissues using an RNAprep Pure Plant Plus Kit (TIANGEN, DP441). Library preparation was as described in our previous study (Sun et al., 2020).

The mobile mRNA transcripts were derived from grafted (and un-grafted) scion or rootstock samples and compared with the reference genome (ftp://ftp.bioinfo.wsu.edu/ species/Malus_x_domestica/Malus_x_domestica-genome_GDDH13_version 1.1/assembly) using the HISAT2 software (Gao et al., 2011; https://ccb.jhu.edu/software/hisat2/index.shtml). Before comparing to the reference genome, we determined four groups of sequences (nongrafted, *Md*/*Mn* 0 h, +Fe *Md*/*Mn*, and −Fe *Md*/*Mn*) using the rootstocks and scion raw data, referred to as reference I, II, III, and IV, respectively. These sequences were first compared to the reference genome, and unmapped reads were removed. To identify leaf to root mobile transcripts, we compared *Mn* (r) versus *Md*/*Mn* (r) (*Mn*: *Mx* or *Mb*, r: root, L: leaf), and searched for SNPs and InDels (insertion–deletions) using *Mn* (r) as control. SNP/InDels detected in *Md*/*Mn* (r) but not in *Mn* (r) were considered as candidates for transmission from the leaf to the root in *Md*/*Mn*. Similar criteria were used to identify candidates for transmission from the root to the leaf. To identify mobile transcripts in response to Fe deficiency, we compared the SNP/indels in sequences from *Md*/*Mn* (r) grown under normal Fe conditions with those from sequences grown under Fe-deficiency conditions. SNPs and InDels were identified and mapped to the apple genome using Genome Analysis Toolkit (GATK;http://www.broadinstitute.org/gatk/). The GATK identification criteria used were: (1) No more than three single base mismatches in the range of 35 bp; (2) Compared with the reference genome, all unique loci in the grafted sample had a sequencing depth >2.0 and two replicates were retained for further analysis. The snpEff software was used for annotation, and only homozygous variants were kept for further analysis. An overview of the methods used in our study is showed in Figure 1, C and D.

Reverse transcription quantitative PCR

First-strand cDNA was synthesized using HiScript® II Q RT SuperMix for qPCR (Vazyme, Nanjing, China; R232-01). RT-qPCR was performed using an ABI QuantStudio™ 6 Flex system (ThermoFisher Scientific, Waltham, MA, USA) with a SensiFAST™ SYBR Lo-ROX Kit (Bioline, London, UK; BIO-94005) For reverse transcription quantitative PCR (RT-qPCR), the thermocycler protocol was as follows: predenaturation, 1 min at 95°C, 40 cycles of 95°C for 15 s, 56°C for 15 s, and 72°C for 45 s. ACTIN (*Md*) was used as reference gene, and the relative expression levels were calculated using the $2^{-\Delta\Delta CT}$ method (Livak and Schmittgen 2001). Primers used are listed in Supplemental Table S3.

RNA FISH of *OPT3*

The roots and stems of hydroponically grown *Md* seedlings were used as RNA FISH experimental materials. The roots and stems of ∼1-cm long were fixed as described previously (Yang et al., 2020). The samples were then dehydrated and buried in paraffin (Yang et al., 2016). A slicer was used to cross-cut the tissue into 8-μm slices. The treatment on these slices, that is, dewaxing, rehydration, and dehydration, followed a previous study (Yang et al., 2016). The probe labeled with 5-Carboxyfluorescein (FAM) was synthesized by Gefan Biological Co., Ltd. (Shanghai, China). The sequence of the probe is shown in Supplemental Table S3. Hybridization is the same as described previously (Yang et al., 2016). During hybridization, FAM-labeled probe was used to react with the sample in the dark at 65°C for 48 h. The nuclei were stained with 4′,6-diamidino-2-phenylindole staining solution for 5 min, and then the sections were processed and sealed. The image was taken with OLYMPUS FV3000 confocal microscope.

Perls' staining

$K_4[Fe(CN)_6]$:HCl = 1:1 (Perls') was used to visualize Fe^{3+} localization as previously described (Meguro et al., 2007). The roots and leaves of transient transgenic *Md* were incubated tin the Perls' solution for 1 h then washed with water. A methanol solution containing 10 mM sodium azide and 0.3% (v/v) H_2O_2 was used to clear the roots and leaves. The samples were then washed in 0.1 M phosphate-buffered saline solution (composed of NaH_2PO_4 and Na_2HPO_4, pH 7.4).

Cloning and sequencing of *OPT3*

A 5′ and 3′ Rapid Amplification of cDNA Ends procedure was used to confirm the full-length mRNA sequence of *MdOPT3*, *MxOPT3*, and *MbOPT3* as previously described (Scotto-Lavino et al., 2006a, 2006b). In order to confirm the stable SNPs, the full-length coding sequence (CDS) of *MdOPT3*, *MxOPT3*, and *MbOPT3* were cloned from cDNA reverse transcribed from total mRNA using the pTOPO-Blunt Cloning vector (AidLab, CV15). All primers are listed in Supplemental Table S3.

SNP typing

To study the mRNA mobility of *MdOPT3*, *MxOPT3*, and *MbOPT3*, we detected the stable SNP of *OPT3* in the roots and leaves of *Mx*/*Md*, *Mb*/*Md*, *Md*/*Mb*, and *Md*/*Mx* grafted seedlings under +Fe and −Fe treatments. SNP typing was completed by Sangon Biotec Co., Ltd (Shanghai, China).

Transient expression

To study the *OPT3* mobility in *Malus* and Arabidopsis, the mRNA sequence of *MdOPT3 and AtOPT3* were separately cloned into the BamH1 site of the pRI101-AN vector. To completement the *Atopt3* by the *MdOPT3*, the promoter sequence of *AtOPT3* and mRNA sequence of *MdOPT3* were cloned into the BamH1 site of the pCAMBIA1391 vector. To increase the abundance of MdRBP in leaf CCs, the promoter sequence of *AtSUC2* and CDS of *MdRBP* were cloned into pCAMBIA1391 in tandem. To suppress *MdOPT3* expression in "Golden Delicious" using virus-induced gene silencing, the *MdOPT3* fragment (Supplemental Table S3) was cloned into the pTRV2 vector (Ramegowda et al., 2014).

All constructs were transformed into GV3101 *Agrobacterium tumefaciens* cells (Weidi Biotechnology, Nanjing, China; AC1001). Positive clones were mixed to give equal concentrations of pTRV1 (Liu et al., 2002) and pTRV2, or its derivatives, and introduced into *Md* and *A. thaliana* seedlings using vacuum infiltration and injection, respectively (Sun et al., 2020). The transformation procedure used a pressure of 0.8 MPa, which was applied twice for 5-min duration. Distilled water was used to wash away the bacteria on the surface of the seedlings.

RNA–protein pull down and mass spectrometry

The *MdOPT3* 3′-UTR fragment was fused with T7 promoter sequence at both ends by PCR. About 2 μg of PCR products were transcribed in vitro using in vitro Transcription T7 Kit (TaKaRa, Shiga, Japan; 6140) kit. The integrity of transcripts was checked by agarose gel electrophoresis. Proteins were extracted from apple plant seedlings using the Plant Total Protein Extraction Kit (Sangon, Shanghai, China; C500053). The target RNAs were labeled using the Thermo Scientific Pierce RNA 3'Desthiobiotinylation Kit (Thermo Scientific, Waltham, MA, USA; 20163). The successive steps of RNA attachment to magnetic beads, incubation in the buffer, elution of RNA–protein complex, and final mass spectrometry detection all follow the Pierce Magnetic RNA–Protein Pull-Down Kit (Thermo Scientific; 20164). RNA–protein complex was detected by Q Exactive HF-X sequencer. The mass-charge ratio of peptides and peptides was collected according to the following method: Twelve fragment profiles (mass spectrometry 2 scan) were acquired after each full scan (mass spectrometry1 scan), MS1 scan in profile mode with a resolution of 70,000 and MS2 scan in profile mode with a resolution of 17,500. Collision energy: 27.0%, isolation window: 1.2 m/z. window: 1.2 *m*/z. The MaxQuant version 1.6.0.16 software was used to analyze the original data file (raw file). Maxquant's algorithm was used to identify peptides and proteins, and gave the relative quantitative information (LFQ). After obtaining the proteins bound to the *MdOPT3* 3′-UTR, we used http://bioinformatics.cau.edu.cn/AppleMDO/ for functional annotation and GO enrichment analysis of target proteins.

SPR

The 3′-UTR RNA probes of *MdOPT3*, *MxOPT3*, and *AtOPT3* were transcribed using the In vitro Transcription T7 Kit (Takara, Shiga, Japan; 6140). The GST-tagged RBPs were expressed using the pGEX4T-1 prokaryotic expression vector (cwbiotech, Beijing, China; CW2198) in *E. coli* BL21 (Transgen, Strasbourg, France; CD901-02). SPR measurements were performed using the GST Capture Kit on the Biacore X100 platform (GE Healthcare Chicago, IL, USA). RNA and RBP binding levels were tested using a Biacore Binding Analysis program (GE Healthcare) with purified RNA probes as the mobile phase, and GST-tagged RBPs as the stationary phase. Binding level is defined as the value of the binding number of the Reaction Unit given by the binding analysis program after the stable combination of the sample and the fixed phase.

Statistical analysis

For all multiple comparisons, GraphPad Prism software (https://www.graphpad.com) was used to analyze the significance of the differences between different groups through a one-way analysis of variance with a significance level of 0.01 and 0.05. * Represents $P < 0.05$, and ** represents $P < 0.01$.

Accession numbers

Sequence data from this article can be found in the GDR and TAIR data libraries under the following accession numbers: *MdOPT3* (MD00G1163400), *MdIRT1* (MD05G1255500), *MdFRO2* (MD01G1068200), *MdFIT* (MD03G1129100), *AtOPT3* (AT4G16370.1), *AtIRT1* (AT4G19690.2), *AtFRO2* (AT1G01580.1), and Fe-deficiency-induced transcription factor 1 (*AtFIT*; AT2G28160.1). RNA-seq data has been uploaded to the NCBI public database (SRP071838)

Supplemental data

The following materials are available in the online version of this article.

Supplemental Method S1. Plant materials.

Supplemental Method S2. SNPs between different samples were used to identify transmissible mRNAs.

Supplemental Method S3. Transient expression.

Supplemental Method S4. Ferric-chelate reduction activity.

Supplemental Figure S1. Spatiotemporal differential expression and GO enrichment analysis of mobile mRNAs in response to Fe stress.

Supplemental Figure S2. Weighted gene co-expression network analysis (WGCNA) of *Malus* mobile mRNAs associated with responses to Fe deficiency.

Supplemental Figure S3. *AtOPT3 and MdOPT3* have different transmissibility in *P. tremula and S. lycopersicum*.

Supplemental Figure S4. A mobile mRNA *AtTCTP1* in *A. thaliana* can move from shoot to root in Arabidopsis seedlings grafted WT/*opt3-2*.

Supplemental Figure S5. Inhibiting the expression of (*Md*) RBP (*MdRBP*) in leaves could block the movement of *MdOPT3* mRNA from *Malus* leaves to roots.

Supplemental Figure S6. Transient overexpression of ProSUC2::*MdRBP* in the leaves of Arabidopsis seedlings grafted WT/*opt3-2* could promote the mobility of *AtOPT3* from shoot to root.

Supplemental Figure S7. The RRM domain of *MdRBP* in herbaceous and woody plants.

Supplemental Figure S8. *OPT3* in both *Malus and A. thaliana* responds to Fe-deficiency stress.

Supplemental Figure S9. Transient overexpression of *MdOPT3* in Arabidopsis *opt3-2* mutant leaves can complement part of the phenotype of *opt3-2*.

Supplemental Figure S10. There are differences in mobility between *MbOPT3 and MxOPT3*.

Supplemental Figure S11. GO Analysis of WT versus *opt3-2* in *A. thaliana* and TRV-*MdOPT3* versus Control in *Malus* seedlings.

Supplemental Figure S12. The secondary structure of *AtOPT3* 3′-UTR sequence.

Supplemental Table S1. Total mobile mRNAs in response to Fe treatment.

Supplemental Table S2. List of genes associated with *OPT3* in WGCNA.

Supplemental Table S3. Primers used in this study.

Supplemental Table S4. Protein annotation of *MdOPT3* 3′ UTR sequence interactors identified in an RNA–protein pull-down analysis.

Supplemental Table S5. DEG and GO analysis of TRV-*MdOPT3* versus Control and WT versus *opt3-2*.

Funding

This work was supported by the National Natural Science Foundation of China (No. 31572097), the China Agricultural Research System (CARS-27), the Construction of Beijing Science and Technology Innovation and Service Capacity in Top Subjects (CEFF-PXM2019_014207_000032), the 111 Project (B17043), and the 2115 Talent Development Program of China Agricultural University.

Conflict of interest statement. The authors declare that the research was conducted in the absence of any commercial or financial relationships that could be construed as a potential conflict of interest.

References

Aloni B, Cohen R, Karni L, Aktas H, Edelstein M (2010) Hormonal signaling in rootstock-scion interactions. Sci Hortic **127**: 119–126

Aoki K, Suzui N, Fujimaki S, Dohmae N, Yonekura-Sakakibara K, Fujiwara T, Hayashi H, Yamaya T, Sakakibara H (2005) Destination-selective long-distance movement of phloem proteins. Plant Cell **17**: 1801–1814

Banerjee AK, Chatterjee M, Yu YY, Suh SG, Miller WA, Hannapel DJ (2006) Dynamics of a mobile RNA of potato involved in a long-distance signaling pathway. Plant Cell **18**: 3443–3457

Brear EM, Day DA, Smith PMC (2013) Iron: an essential micronutrient for the legume-rhizobium symbiosis. Front Plant Sci **4**: 359

Chen XB, Yao QF, Gao XH, Jiang CF, Harberd NP, Fu XD (2016) Shoot-to root mobile transcription factor HY5 coordinates plant carbon and nitrogen acquisition. Curr Biol **5**: 640–646

Cho SK, Sharma P, Butler NM, Kang IH, Shah S, Rao AG, Hannapel DJ (2015) Polypyrimidine tract-binding proteins of potato mediate tuberization through an interaction with *StBEL5* RNA. J Exp Bot **66**: 6835–6847

Duan XW, Zhang WN, Huang J, Hao L, Wang SN, Wang AD, Meng D, Zhang QL, Chen QJ, Li TZ (2015) *PbWoxT1* mRNA from pear (*Pyrus betulaefolia*) undergoes long-distance transport assiated by a polypyrimidine tract binding protein. New Phytol **210**: 511–524

Edelstein M, Ben-Hur M, Cohen R, Burger Y, Ravina I (2005) Boron and salinity effects on grafted and non-grafted melon plants. Plant Soil **269**: 273–284

Endo S, Betsuyaku S, Fukuda H (2014) Endogenous peptide ligand-receptor systems for diverse signaling networks in plants. Curr Opin Plant Biol **21**: 140–146

Enomoto Y, Hodoshima H, Shimada H, Shojo K, Yoshihara T, Goto F (2007) Long-distance signals positively regulate the expression of iron uptake genes in tobacco roots. Planta **227**: 81–89

Ferrandon D, Elphick L, Nussleinvolhard C, Stjohnston D (1994) Staufen protein associates with the 3′ UTR of bicoid messenger-RNA to form particles that move in a microtubule-dependent manner. Cell **79**: 1221–1232

Gao C, Wang Y, Xiao DS, Qiu CP, Han DG, Zhang XZ, Wu T, Han ZH (2011) Comparison of cadmium-induced iron-deficiency responses and genuine iron-deficiency responses in *Malus xiaojinensis*. Plant Sci **181**: 269–274

Garcia MJ, Romera FJ, Stacey MG, Stacey G, Villar E, Alcantara E, Perez-Vicente R (2013) Shoot to root communication is necessary to control the expression of iron-acquisition genes in Strategy I plants. Planta **237**: 65–75

Grillet L, Lan P, Li WF, Mokkapati G, Schmidt W (2018) IRON MAN is a ubiquitous family of peptides that control iron transport in plants. Nat Plants **4**: 953–963

Grusak MA, Pezeshgi S (1996) Shoot-to-root signal transmission regulates root Fe(III) reductase activity in the dgl mutant of pea. Plant Physiol **110**: 329–334

Ham BK, Brandom JL, Xoconostle-Cazares B, Ringgold V, Lough TJ, Lucas WJ (2009) A polypyrimidine tract binding protein, pumpkin RBP50, forms the basis of a phloem-mobile ribonucleoprotein complex. Plant Cell **21**: 197–215

Ham BK, Lucas WJ (2017) Phloem-mobile RNAs as systemic signaling agents. Annu Rev Plant Biol **68**: 173–195

Han ZH, Wang Q, Shen T (1994) Comparison of some physiological and biochemical characteristics between iron-efficient and iron-inefficient species in the *genus Malus*. J Plant Nutr **17**: 1257–1264

Hannapel DJ (2010) A model system of deve development regulated by the long-distance transport of mRNA. J Integr Plant Biol **52**: 40–52

Hansch R, Mendel RR (2009) Physiological functions of mineral micronutrients (Cu, Zn, Mn, Fe, Ni, Mo, B, Cl). Curr Opin Plant Biol **12**: 259–266

Haywood V, Yu TS, Huang NC, Lucas WJ (2005) Phloem long-distance trafficking of gibberellic acid-insensitive RNA regulates leaf development. Plant J **42**: 49–68

Hu CY, Ham BK, El-Shabrawi HM, Alexander D, Zhang DB, Ryals J, Lucas WJ (2016) Proteomics and metabolomics analyses reveal the cucurbit sieve tube system as a complex metabolic space. Plant J **87**: 442–454

Kehr J, Buhtz A (2008) Long distance transport and movement of RNA through the phloem. J Exp Bot **59**: 85–92

Kehr J, Kragler F (2018) Long distance RNA movement. New Phytol **218**: 29–40

Khan MA, Castro-Guerrero NA, McInturf SA, Nguyen NT, Dame AN, Wang JJ, Bindbeutel RK, Joshi T, Jurisson SS, Nusinow, DA, et al. (2018) Changes in iron availability in Arabidopsis are rapidly sensed in the leaf vasculature and impaired sensing leads to opposite transcriptional programs in leaves and roots. Plant Cell Environ **41**: 2263–2276

Kim G, LeBlanc ML, Wafula EK, Depamphilis CW, Westwood JH (2014) Genomic-scale exchange of mRNA between a parasitic plant and its hosts. Science **345**: 808–811

Kobayashi T, Nishizawa NK (2012) Iron uptake, translocation, and regulation in higher plants. Annu Rev Plant Biol **63**: 131–152

LeBlanc M, Kim G, Patel B, Stromberg V, Westwood J (2013) Quantification of tomato and Arabidopsis mobile RNAs trafficking into the parasitic plant *Cuscuta pentagona*. New Phytol **200**: 1225–1233

Lin MK, Lee YJ, Lough TJ, Phinney BS, Lucas WJ (2009) Analysis of the pumpkin phloem proteome provides insights into angiosperm sieve tube function. Mol Cell Proteomics **8**: 343–356

Liu YL, Schiff M, Marathe R, Dinesh-Kumar SP (2002) Tobacco *Rar1*, *EDS1* and *NPR1/NIM1* like genes are required for N-mediated resistance to tobacco mosaic virus. Plant J **30**: 415–429

Livak KJ, Schmittgen TD (2001) Analysis of relative gene expression data using real-time quantitative PCR and the $2_{T}^{-\Delta\Delta C}$ method. Methods **25**: 402–408

Lubkowitz M (2011) The oligopeptide transporters: a small gene family with a diverse group of substrates and functions. Mol Plant **4**: 407–415

Luo WG, XiaoY, Liang QW, Su Y, Xiao LT (2019) Identification of potential auxin-responsive small signaling peptides through a peptidomics approach in *Arabidopsis thaliana*. Molecules **24**: 3146

Mai HJ, Pateyron S, Bauer P (2016) Iron homeostasis in *Arabidopsis thaliana*: transcriptomic analyses reveal novel FIT-regulated genes, iron deficiency marker genes and functional gene networks. BMC Plant Biol **16**: 211

Marsch MN, Frankan J, Gonzalez KL, Folter S, Angenent G, Alvarez ER. (2013) An efficient flat-surface collar-free grafting method for *Arabidopsis thaliana* seedlings. Plant Methods **9**: 14

Meguro R, Asano Y, Odagiri S, Li CT, Iwatskui H, Shoumura K (2007) Nonheme-iron histochemistry for light and electron microscopy: a historical, theoretical and technical review. Arch Histol **70**: 1–19

Melnyk CW (2017) Plant grafting: insights into tissue regeneration. Regeneration (Oxf) **4**: 3–14

Mendoza-Cozatl DG, Xie QQ, Akmakjian GZ, Jobe TO, Patel A, Stacey MG, Song L, Demoin DW, Jurisson SS, Stacey G, et al. (2014) OPT3 is a component of the iron-signaling network between leaves and roots and misregulation of OPT3 leads to an over-accumulation of cadmium in seeds. Mol Plant **7**: 1455–1469

Molnar A, Melnyk CW, Bassett A, Hardcastle TJ, Dunn R, Baulcombe DC (2010) Small silencing RNAs in plants are mobile and direct epigenetic modification in recipient cells. Science **328**: 872–875

Morris RJ (2018) On the selectivity, specificity and signalling potential of the long-distance movement of messenger RNA. Curr Opin Plant Biol **43**: 1–7

Murphy E, Smith S, DeSmet I (2012) Small signaling peptides in Arabidopsis development: how cells communicate over a short distance. Plant Cell **24**: 3198–3217

Papadakis IE, Dimassi KN, Bosabalidis AM, Therios IN, Patakas A, Giannakoula A (2004a) Boron toxicity in 'Clementine' mandarin plants grafted on two rootstocks. Plant Sci **166**: 539–547

Papadakis IE, Dimassi KN, Bosabalidis AM, Therios IN, Patakas A, Giannakoula A (2004b) Effects of B excess on some physiological and anatomical parameters of 'Navelina' orange plants grafted on two rootstocks. Environ Exp Bot **51**: 247–257

Ramegowda V, Mysore KS, Senthil-Kumar M (2014) Virus-induced gene silencing is a versatile tool for unraveling the functional relevance of multiple abiotic-stress-responsive genes in crop plants. Front Plant Sci **5**: 323

Rivero RM, Ruiz JM, Romero L (2003) Can grafting in tomato plants strengthen resistance to thermal stress? J Sci Food Agric **83**: 1315–1319

Rodriguez-Medina C, Atkins CA, Mann AJ, Jordan ME, Smith PMC (2011) Macromolecular composition of phloem exudate from white lupin (*Lupinus albus L.*). BMC Plant Biol **11**: 36

Sanchez-Rodriguez E, Leyva R, Constan-Aguilar C, Romero L, Ruiz JM (2012) Grafting under water stress in tomato cherry: improving the fruit yield and quality. Ann Appl Biol **161**: 302–312

Scotto-Lavino E, Du GW, Frohman MA (2006a) 5' end cDNA amplification using classic RACE. Nat Protoc **1**: 2555–2562

Scotto-Lavino E, Du GW, Frohman MA (2006b) 3' End cDNA amplification using classic RACE. Nat Protoc **1**: 2742–2745

Singh G, Pratt G, Yeo GW, Moore MJ (2015) The clothes make the mRNA: past and present trends in mRNP fashion. Annu Rev Biochem **84**: 325–354

Stacey MG, Koh S, Becker J, Stacey G (2002) AtOPT3, a member of the oligopeptide transporter family, is essential for embryo development in Arabidopsis. Plant Cell **14**: 2799–2811

Stacey MG, Pater A, McClain WE, Mathieu M, Remley M, Rogers EE, Gassmann W, Blevins DG, Stacey G (2008) The Arabidopsis AtOPT3 protein functions in metal homeostasis and movement of iron to developing seeds. Plant Physiol **146**: 589–601

Stacey MG, Osawa H, Patel A, Gassmann W, Stacey G (2006) Expression analyses of Arabidopsis oligopeptide transporters during seed germination, vegetative growth and reproduction. Planta **223**: 291–305

Sun YQ, Hao PB, Lv XM, Tian J, Wang Y, Zhang XZ, Xu XF, Han ZH, Wu T (2020) A long non-coding apple RNA, MSTRG.85814.11, acts as a transcriptional enhancer of SAUR32 and contributes to the Fe-deficiency response. Plant J **103**: 53–67

Taller J, Hirata Y, Yagishita N, Kita M, Ogata S (1998) Graft-induced genetic changes and the inheritance of several characteristics in pepper (*Capsicum annuum* L.). Theor Appl Genet **97**: 705–713

Taoka K, Ham BK, Xoconostle-Cazares B, Rojas MR, Lucas WJ (2007) Reciprocal phosphorylation and glycosylation recognition motifs control NCAPP1 interaction with pumpkin phloem proteins and their cell-to-cell movement. Plant Cell **19**: 1866–1884

Thieme CJ, Rojas-Triana M, Stecyk E, Schudoma C, Zhang W, Yang L, Miñambres M, Walther D, Schulze WX, Paz-Ares J, et al. (2015) Endogenous Arabidopsis messenger RNAs transported to distant tissues. Nat Plants **1**: 4

Venema JH, Dijk BE, Bax JM, van Hasselt PR, Elzenga JTM (2008) Grafting tomato (*Solanum lycopersicum*) onto the rootstock of a high-altitude accession of Solanum habrochaites improves suboptimal-temperature tolerance. Environ Exp Bot **63**: 359–367

Wang J, Jiang LB, Wu RL (2017) Plant grafting: how genetic exchange promotes vascular reconnection. New Phytol **214**: 56–65

Warschefsky EJ, Klein LL, Frank MH, Chitwood DH, Londo JP, von Wettberg EJ, Miller AJ (2015) Rootstocks: diversity, domestication, and impacts on shoot phenotypes. Trends Plant Sci **21**: 418–437

Wu T, Zhang HT, Wang Y, Jia WS, Xu XF, Zhang XZ, Han ZH (2012) Induction of root Fe(III) reductase activity and proton extrusion by iron deficiency is mediated by auxin-based systemic signalling in *Malus xiaojinensis*. J Exp Bot **63**: 859–870

Xia C, Zheng Y, Huang J, Zhou X, Li R, Zha M, Wang S, Huang Z, Lan H, Turgeon R et al. (2018) Elucidation of the mechanisms of long-distance mRNA movement in a *Nicotiana benthamiana*/tomato heterograft system. Plant Physiol **177**: 745–758

Xia C, Zhang CK (2020) Long-distance movement of mRNAs in plants. Plants **9**: 731

Xoconostle-Cazares B, Yu X, Ruiz-Medrano R, Wang HL, Monzer J, Yoo BC, McFarland KC, Franceschi VR, Lucas WJ (1999) Plant paralog to viral movement protein that potentiates transport of mRNA into the phloem. Science **283**: 94–98

Yang L, Perrera V, Saplaoura E, Apelt F, Bahin M, Kramdi A, Olas J, Mueller-Roeber B, Sokolowska E, Zhang WN, et al. (2019) m5C methylation guides systemic transport of messager RNA over graft junctions in plants. Curr Biol **29**: 2465–2476

Yang W, Schuster C, Beahan CT, Charoensawan V, Peaucelle A, Bacic A, Doblin MS, Wightman R, Meyerowitz EM (2016) Regulation of meri-stem morphogenesis by cell wall synthases in *Arabidopsis*. Curr Biol **26**: 1404–1415

Yang WB, Schuster C, Prunet N, Dong QK, Landrein B, Wightman R, Meyerowitz EM (2020) Visualization of protein coding, long noncoding, and nuclear RNAs by fluorescence in situ hybridization in sections of shoot apical meristems and developing flowers. Plant Physiol **182**: 147–158

Yang YZ, Mao LY, Jittayasothorn Y, Kang YM, Jiao C, Fei ZJ, Zhong GY (2015) Messenger RNA exchange between scions and rootstocks in grafted grapevines. BMC Plant Biol **15**: 251

Zhai ZY, Gayomba SR, Jung H, Vimalakumari NK, Piñeros M, Craft E, Rutzke MA, Danku J, Lahner B, Punshon T, et al. (2014) OPT3 is a phloem-specific iron transporter that is essential for systemic iron signaling and redistribution of iron and cadmium in Arabidopsis. Plant Cell **26**: 2249–2264

Zhang ML, Lv YD, Wang Y, Rose JKC, Shen F, Han ZY, Zhang XZ, Xu XF, Wu T, Han ZH (2017) TATA box insertion provides a selection mechanism underpinning adaptations to Fe deficiency. Plant Physiol **173**: 715–727

Zhang WN, Thieme CJ, Kollwig G, Apelt F, Yang L, Winter N, Andresen N, Walther D, Kragler F (2016a) tRNA-related sequences trigger systemic mRNA transport in plants. Plant Cell **28**: 1237–1249

Zhang ZL, Zheng Y, Ham BK, Chen JY, Yoshida A, Kochian LV, Fei ZJ, Lucas WJ (2016b) Vascular-mediated signalling involved in early phosphate stress response in plants. Nat Plants **2**: 4